Available online at www.sciencedirect.com
SCIENCE DIRECT®
Journal of Hydrology 325 (2006) 56–66
Journal of Hydrology
www.elsevier.com/locate/jhydrol

# Characterization of temporal variability in near-surface soil moisture at scales from 1 h to 2 weeks

Annie-Claude Parent [a], François Anctil [a,*], Léon-Étienne Parent [b]

[a] *Département de génie civil, Pavillon Adrien-Pouliot, Université Laval, Sainte-Foy, Qué., Qc, Canada G1K 7P4*
[b] *Département de sols et de génie agroalimentaire, Pavillon Comtois, Université Laval, Qué., Qc, Canada G1K 7P4*

Received 4 March 2005; revised 26 September 2005; accepted 29 September 2005

**Abstract**

This study proposes a characterization of the temporal relations between soil moisture and precipitation at a very short time-scale, i.e. from 1 h to 2 weeks. The analysis is based on seven soil moisture time series from time domain transmission (TDT) probes positioned along a 90-m transect, and monitored at a 20-min rate in the shallow soil layer (5–25 cm), and on precipitation observed every 15 min. Wavelet analysis is proposed for the characterization of the temporal relationships between soil moisture and precipitation. The normalized local wavelet spectrum of soil moisture reveals power features related to the precipitation events in the short scales, and residing in the long scales. The variance activity depicted in the wavelet power spectra of precipitation and soil moisture is organized in preferential bands of wavelet scales: 1–48 h, 48 h to 1 week, and 1–2 weeks. For the 1–48 h scale, soil moisture is linked to precipitation occurrence, intensity and duration, while for the 48 h to 1 week scale soil moisture relates to the periodicity of the rainfall events, and for the 1–2 weeks scale to the duration of the dry spells. Additionally, a distance–time wavelet analysis was conducted to simultaneously assess spatial and temporal variabilities for each of the three predefined bands. The spatial analysis showed many similarities between series along the transect that were attributable to soil homogeneity. The averaging of the variance showed that 93% of the concentration of the precipitation variance was at the 1–48 h scale, while most of the soil moisture variation (85%) was accounted for at the 48 h to 2 weeks scale. Disparity between the short duration of precipitation system and the extension of the soil moistening process is due to the transfer of energy from precipitation to soil moistening.


*Keywords:* Soil moisture; Wavelet analysis; Temporal variability, Principal component analysis

## 1. Introduction

Near surface soil moisture variations influence the ecosystem response to changes in the physical environment over a large range of spatial and temporal scales, particularly the partitioning of available energy at ground surface into sensible and latent heat. Such partitioning drives not only vertical fluxes of energy and moisture, but also nearly horizontal fluxes of moisture, namely, runoff. Variations in drought, flood, and surface temperature are linked to soil moisture dynamics, a determinant

* Corresponding author. Tel.: +1 418 656 3653; fax: +1 418 656 2928.
*E-mail address:* francois.anctil@gci.ulaval.ca (F. Anctil).

0022-1694/$ - see front matter © 2006 Elsevier B.V. All rights reserved.
doi:10.1016/j.jhydrol.2005.09.027

parameter in climate modelling. A negative water balance at some key period during plant growth may affect potential crop yields. Soil water content is an essential parameter for crop growth and yield forecasting in deterministic models, as well as for monitoring water stress detection and irrigation management.

How soil moisture responds to atmospheric forcing factors varies in time and space. Available observation networks of soil moisture have been examined by Vinnikov et al. (1996); Entin et al. (2000) to evaluate scale effects. They partitioned the variance into two components: a fine scale, influenced by soils, topography, and vegetation, and a large scale driven by climate. Besides a few large databases, systematic observations of soil moisture content are scarce (Georgakakos and Baumer, 1996), especially because gravimetric techniques, neutron probe, and time domain reflectometry or transmission are labour intensive and therefore cannot be reasonably implemented to routinely monitor extended areas. As a result, ground measurements usually provide data that are easily calibrated, but only cover small areas with few repetitions (weekly time steps in the best cases), hence limiting the accessible scale of temporal variability to an intra-seasonal time step at the shortest.

The analysis conducted in this work follows and extends that of Wu et al. (2002); Lauzon et al. (2004), focusing on temporal characterization of soil moisture time series and on the linkage between soil moisture and supporting data such as precipitation. Wu et al. (2002) quantified, using observations for a 16-year period across the state of Illinois (10-day time step), the low-pass filter climatology of soil hydrology in terms of amplitude damping, phase shifting, and increasing persistence with soil depth. Their analysis confirmed that the annual to seasonal cycles are the leading modes of variation for the soil moisture profile. At a finer temporal scale, based on a 3.5-year period for the Orgeval watershed in France (12-h time step), Lauzon et al. (2004) showed that soil moisture accounted for the annual cycle present in the observed flows (in that region precipitation shows no annual cycle). The links between precipitation events, the short-term behaviour of soil moisture and the inflow regime was also established. A distinctive element of the present study is its database, which contains soil moisture observations taken at a 20-min time step and rainfall observation taken at a 15-min time step, hence allowing the study of temporal variability at very short time scales.

Wavelet analysis is proposed for the characterization of seven soil moisture time series, along a 90-m transect, and for the identification of temporal relationships between soil moisture and precipitation. Wavelet transform departs from Fourier transform in that it accepts changes in spectral power properties over time, and can account for both time and spatial domains. Soil moisture similarities are first explored through data reduction based on principal component analysis. Thereafter, spatial differences are investigated through distance–time diagrams for pertinent wavelet-scale bands.

In Section 2, the context of application is presented: experimental site, observations, and data reduction analysis. Section 3 provides a technical background on wavelet analysis. Section 4 presents results. A discussion and a conclusion based on the relevant findings of this work are given in Sections 5 and 6.

## 2. Context of application

### 2.1. Experimental site

The experiment was performed in southern Québec, Canada, on a crop field located at Saint-Ubalde (latitude 46°N, longitude 72°W). This region has a temperate climate, a mean temperature of 15 °C, and an average monthly rainfall of 100 mm in summer. Crop is medium maturing russet potato (*Solanum tuberosum* L.), cultivar Goldrush, that grows from mid-May to mid-September. The soil is an acid ($pH_{CaCl_2,0.01\ M}=4.8$) Morin sandy loam (Haplorthod) containing 23 g C $kg^{-1}$, 65 g clay $kg^{-1}$, and 212 g silt $kg^{-1}$. Owing to a relatively permeable soil material and a constant flat slope of 1° along row direction, the field ensured suitable drainage conditions.

### 2.2. Observations

Soil moisture and precipitation were observed during the growing season from mid-June to August 2003. Soil moisture was monitored 90 m along

a potato row located in the upper-slope part of the field. A set of seven equally spaced probes, using time domain transmission (TDT) technology (e.g. Morari and Giardini, 2002), were installed in the field to measure soil moisture content at a 20-min rate. In TDT, a pulse is emitted from one end of a U-stem and observed at the other end, measuring the time for a wave to be transmitted. The higher the water content, the longer is transmission time. Output is moisture content expressed as a volumetric percentage. In this study, seven probes were installed horizontally into soil between potato plants at a depth of 15 cm, and equally spaced at 15 m from each other. The probes measured water content in the 5–25 cm layer, which corresponds to the detection range of the instruments. The first 30 cm contains most potatoes roots and represents a critical zone for plant water availability. At this depth, water shortage may cause severe stress to the plant that can lead to deceiving tuber yields.

Fig. 1 presents the seven soil moisture time series (8 weeks). Soil moisture ranged from 5 to 25%. The last three graphs, i.e. the 60–90 m sections on the transect, showed a one-week data interruption during the dry spell at the end of June. The missing information was filled by linear interpolation without much loss of information. In parallel, meteorological data were gathered every 15 min from a station in the experimental field.

### 2.3. Data reduction

Principal component analysis (PCA) allows for grouping similar information from several sources of data (Joliffe, 2002), here soil moisture time series

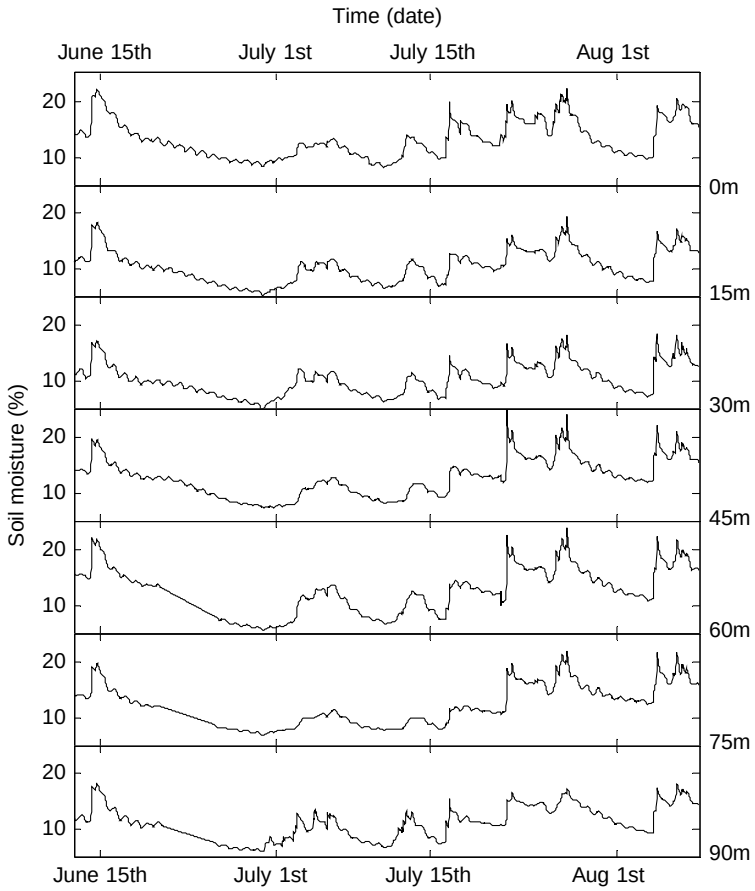


Fig. 1. Soil moisture times series at 20 min intervals for seven TDT probes across a 90-m transect.

obtained from the seven TDT probes. PCA reduces the dimensionality of the soil moisture dataset while retaining as much proportion of the variation as possible. In the present study, a PCA time series of the first principal component (Fig. 2a) was used to identify temporal patterns shared by the seven moisture time series. The first principal component represented 94% of total variance of the time series, while the second and third components accounted only for 3 and 1% of the variance, respectively. Analysis of individual series was used to identify moisture differences between locations.

## 3. Techniques

Wavelet analyses are frequently used in geophysical applications (e.g. Kumar and Foufoula-Georgiou, 1997; Labat et al., 2000) for analysing variance fluctuations within non-stationary time series. Hydrology-related applications include the description of daily streamflow time series (e.g. Smith et al., 1998; Labat et al., 2000; Anctil and Tape, 2004), the analysis of interannual streamflow variability (e.g. Lafrenière and Sharp, 2003; Anctil and Coulibaly, 2004), and the characterization of soil moisture for

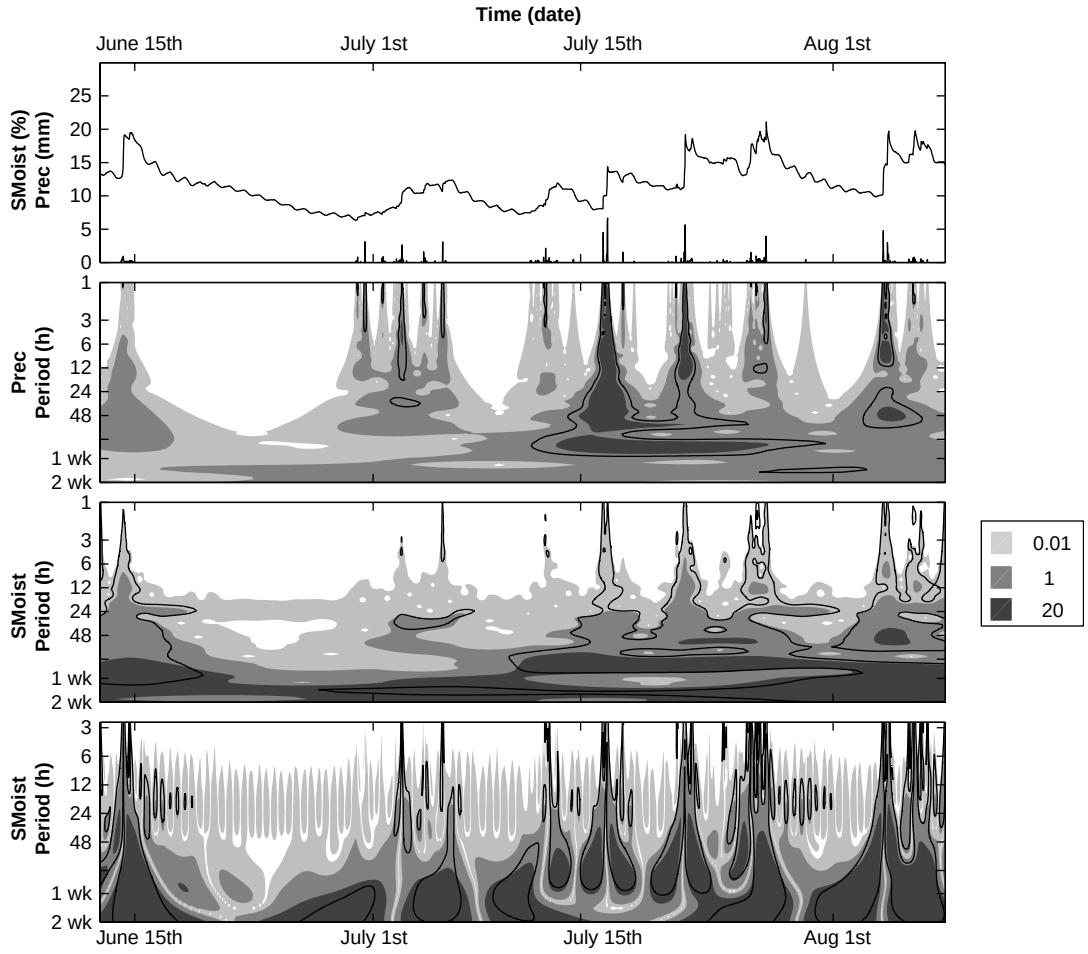


Fig. 2. Window (a) shows the precipitation time series (lower line) and the principal component across the seven soil moisture time series (upper line). Wavelet power spectra of (b) the precipitation time series with Morlet, (c) the soil moisture time series with Morlet and (d) with the Mexican hat. The shaded contours are at normalized variance of 0.01, 1 and 20. The bold contour lines enclose peaks of larger than 95% confidence for a red noise with a lag-1 coefficient $\alpha = 0.58$ for (b) and $\alpha = 1.00$ for (c) and (d).

scales ranging from a few days to a year (Lauzon et al., 2004). Other wavelet applications include the analysis of soil properties (Lark and Webster, 1999; Lark and Webster, 2001), of vegetation density (Cosh and Brutsaert, 2003) and of topographical relationships with crop yields (Si and Farell, 2004). Wavelet analysis, in a geophysical context, has been thoroughly described by Torrence and Compo (1998); Labat et al. (2000).

The continuous wavelet transform $W_n$ of a discrete sequence of observations $x_n$ is defined as the convolution of $x_n$ with a scaled (related to frequency) and translated wavelet $\psi(\eta)$ that depends on a non-dimensional time parameter$\eta$, as follows:

$$W_n^x(s) = \sum_{n'=0}^{N-1} x_{n'} \psi^* \left[ \frac{(n'-n)\delta t}{s} \right], \tag{1}$$

where $n$ is localized time index, $s$ is wavelet scale, $\delta t$ is sampling time interval, $N$ is the number of points in the time series, and the asterisk indicates the complex conjugate. Since complex wavelets lead to complex continuous wavelet transforms, the wavelet power spectrum, defined as $|W_n(s)|^2$, is a convenient description of fluctuation in the variance at different frequencies. Further, power spectrum is normalized by the variance $\sigma^2$ to give a measure of the power relative to white noise since expectation value for a white noise process is $\sigma^2$ at all $n$ and $s$. By normalizing, one ensures that the wavelet transform at each scale $s$ is comparable to each other and to the transforms of other series (Torrence and Compo, 1998).

In the process of wavelet transforms, a large set of wavelet functions may be used. To be admissible, wavelet function must have zero mean and may be represented in both time and frequency domains (Farge, 1992). The selection of one wavelet function depends mainly on data. Other properties are: orthogonal or not, complex or real, width and shape. Refer to Torrence and Compo (1998) for more details on wavelet functions. The most frequently used wavelets in continuous time geophysical applications are known as Morlet and Mexican hat (Malamud and Turcotte, 1999; Labat et al., 2000). The Morlet wavelet is a complex non-orthogonal wavelet consisting of a plane wave modulated by a Gaussian function as follows:

$$\psi_0(\eta) = \pi^{-0.25}\, e^{i\omega_0\eta}\, e^{-0.5\eta^2}, \tag{2}$$

where $\omega_0$ is the non-dimensional frequency, here taken as 6 so as to satisfy the admissibility condition (Farge, 1992; Torrence and Compo, 1998). The real-valued Mexican hat wavelet, which is also non-orthogonal, is defined as a successive derivative of the Gaussian function that returns a single component as follows:

$$\psi_0(\eta) = \frac{(-1)^{m+1}}{\sqrt{\Gamma(2.5)}} \frac{\delta^m}{\delta\eta^m}(e^{-0.5\eta^2}), \tag{3}$$

where the parameter $m=2$. All wavelets express a compromise between their level of temporal and spectral definitions. The strength of Morlet wavelet lies in its spectral definition, while that of Mexican hat wavelet resides in its temporal definition.

When, as in the present study, time series from different locations are available, distance–time diagrams may be drawn to assess spatial and temporal variability in the database. The distance–time diagram, which is composed of scale-averaged wavelet power spectra at multiple locations, is also frequently used to provide variance over selected preferential bands. The scale-averaged wavelet power is defined as the weighted sum of the wavelet power spectrum over scale $s_1$ to $s_2$ as follows:

$$\bar{W}_n^2 = \frac{\delta j \delta t}{C_\delta} \sum_{j=j_1}^{j_2} \frac{|W_n(s_j)|}{s_j}, \tag{4}$$

where $\delta_j$ is a factor for scale resolution (here chosen as 0.1) and $C_\delta$ is a reconstruction factor specific to each wavelet form; $C_\delta = 0.776$ for Morlet and 3.541 for Mexican hat.

## 4. Results

### 4.1. Temporal analysis

Rainfall observations are illustrated in Fig 2a (lower line), while the normalized local Morlet wavelet spectrum of the precipitation time series is displayed in Fig. 2b. In Fig. 2b, the left axis is the equivalent Fourier period corresponding to

the wavelet scale and the bottom axis is time. The shaded contours are the normalized variance in excess of 0.01, 1 and 20. The thick contours enclose peaks of greater than 95% confidence for red noise. In geophysical applications, the red noise remains an appropriate background spectrum in estimating a null hypothesis for the significance of a peak in the wavelet power spectrum (Torrence and Compo, 1998). A lag-1 coefficient $\alpha$ of 0.58 was calculated for this series, following the Monte Carlo analysis of Torrence and Compo (1998) based on the univariate lag-1 autoregressive process. Since the power spectrum associated to a given time series is the result of a natural process producing noise, one should not presume that regions outside these 95% confidence level areas are to be discarded from analysis. The natural process is still present in those regions, but influences the power spectrum to a lesser extent (Nicholls, 2001). The cone of influence described by Torrence and Compo (1998) is absent from Fig. 2b–d, because analyses were performed using finite-length time series (4096 data).

The Morlet power spectrum of precipitation exhibits intermittent high power peaks located in the highest frequencies and some horizontally sketched features at larger scales. The variance distribution shown in Fig. 2b reveals that activity is organized in preferential bands of wavelet scales: 1–48 h, 48 h to 1 week, and 1–2 weeks. Any feature beyond 2 weeks was not considered in this study due to limited duration of the series (8 weeks). Shorter periods ranging from 1 to 48 h exhibit narrow peaks related to precipitation events depicted in Fig. 2a (lower line). Those peaks characterize the power released by each significant rainfall event, and their amplitudes are related to the duration of the event. Features found in longer periods, i.e. more than 48 h, are outcomes from precipitation repeatability that results from local meteorological system periodicity (in the order of 3–7 days).

Precipitation strongly affects soil moisture at shallow depth, where variability over time in soil moisture observations is relatively high, fading out deeper in the soil profile (Lauzon et al., 2004). At depths of 1 m or more, variability over time in soil moisture is rather low, which is characteristic of the role of soil as a buffer, smoothing off gradually the soil moisture signal (Wu et al., 2002). The Morlet power spectrum of soil moisture at Fig. 2c shows much similarities with the precipitation Morlet power spectrum (Fig. 2b), confirming their close relationship. However, the power spectrum of soil moisture enlightens features that are not shown in the precipitation power spectrum, particularly at scales exceeding 1 day (level 20 shaded contours in Fig. 2c). Power peaks for shorter periods (1–48 h) were related to the most important precipitation events, i.e. rainfalls that by their intensity and durability thoroughly moistened the soil. Since surface soil is in direct contact within the atmosphere, major rainfall events are easily identified on Fig. 2c at July 17th, July 20th, July 24th and August 4th. In the same manner, the dry spells in June 15–28th, July 6–12th and July 25th to August 4th, showed up in the soil moisture power spectrum as loss of energy. For longer periods (1–2 weeks), features were attributable to soil rather than precipitation effects. Typically, soil dries and re-moistens more or less rapidly depending of its physical characteristics. In a sandy loam, water drains quickly. Fig. 2c illustrates this process: high frequency peaks related to rainfall events are immediately followed by lacks of energy at low frequencies. A daily pattern is also identifiable. This pattern is related to daily temperature fluctuations. During dry spells or for high moisture conditions, this 24-h periodicity was not defined.

The normalized Mexican hat power wavelet spectrum of soil moisture wavelet is illustrated in Fig. 2d. The temporal scale was more detailed compared to the Morlet wavelet. For instance, soil moisture ups and downs were differentiated by the Mexican hat wavelet function. All major rainfall events produced a pair of power peaks. However, a weakness of the Mexican hat wavelet function is a poorer spectral scale definition due to the vertically lengthened featuring. Also, the definition in high frequencies is limited by the Fourier period which is about eight times the sampling interval. In Fig. 2d, no information is available for scales smaller than 2.66 h (with a time interval of 0.33 h or 20 min). In contrast, the Morlet power spectrum, illustrated in Fig. 2c by enhancing temporal features, provided more details on the time-scale organization of the data, and thus can unravel scale structures.

### 4.2. Distance–time analysis

The distance–time analysis consists of a scale-averaged wavelet power for several time series at multiple locations. In this study, the distance–time analysis was primarily processed to partition the variance into preferential bands, but it was also used to simultaneously assess temporal and spatial variabilities.

The distance–time diagram of soil moisture time series over the 90-m transect is given for three predefined bands, i.e. 1–48 h (Fig. 3a), 48 h to 1 week (Fig. 4a) and 1–2 weeks (Fig. 5a). Those ranges of scales were clearly identified in the soil moisture power spectrum in Fig. 2c as well as in the precipitation power spectrum in Fig. 2b. The distance–time diagrams are depicted in two-dimensional contour plots, with 95% confidence computed using a lag-1 autocorrelation at each site. Alongside each distance–time diagram shown in Figs. 3–5, the zonal average plots for soil moisture and precipitation provided a measure of temporal fluctuations of the series along the transect. For each band, the middle plot presented the zonal average calculated by scale-averaging wavelet power of time series (bold line) and the zonal average calculated using PCA (thin line). Table 1 presents, for the three predefined ranges of scales, how soil moisture and precipitation variances accounted for total variance, and the correlation coefficient between both variables.

The distance–time diagrams revealed many similarities between neighbouring series regardless of scales. Indeed, Figs. 3–5a showed high temporal variability, but low spatial variability due to similarities between original time series (Fig. 1). Although soil water content were homogeneous along the transect, small differences could be detected. Therefore, the distance–time diagram was a powerful tool for conducting a detailed analysis of spatial heterogeneity. Homogeneity observed in this study was attributable to homogeneous soil texture and density, and to uniform drainage and practices. Besides, Figs. 3–5b showed a close correspondence between the scale-averaged wavelet power computed from the time series and the one computed from PCA.

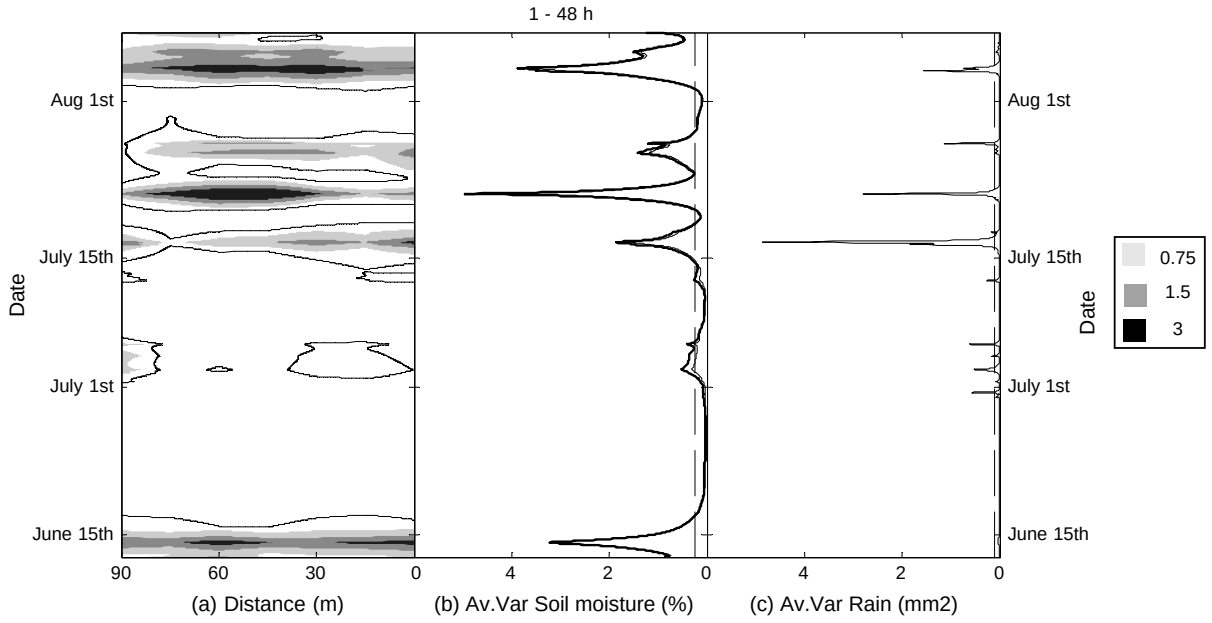


Fig. 3. For band 1–48 h, (a) is the distance–time diagram of soil moisture series. The shaded contours are at normalized variance of 0.75, 1.5 and 3. The bold line is the 95% confidence with lag-1 $\alpha$ coefficient of 1.00. (b) is the scale-averaged wavelet power of soil moisture (bold line is computed from series and thin line is computed from PCA). (c) is the scale-averaged wavelet power of precipitation. Over the dashed line is the 95% confidence with lag-1 $\alpha$ coefficient of 1.00.

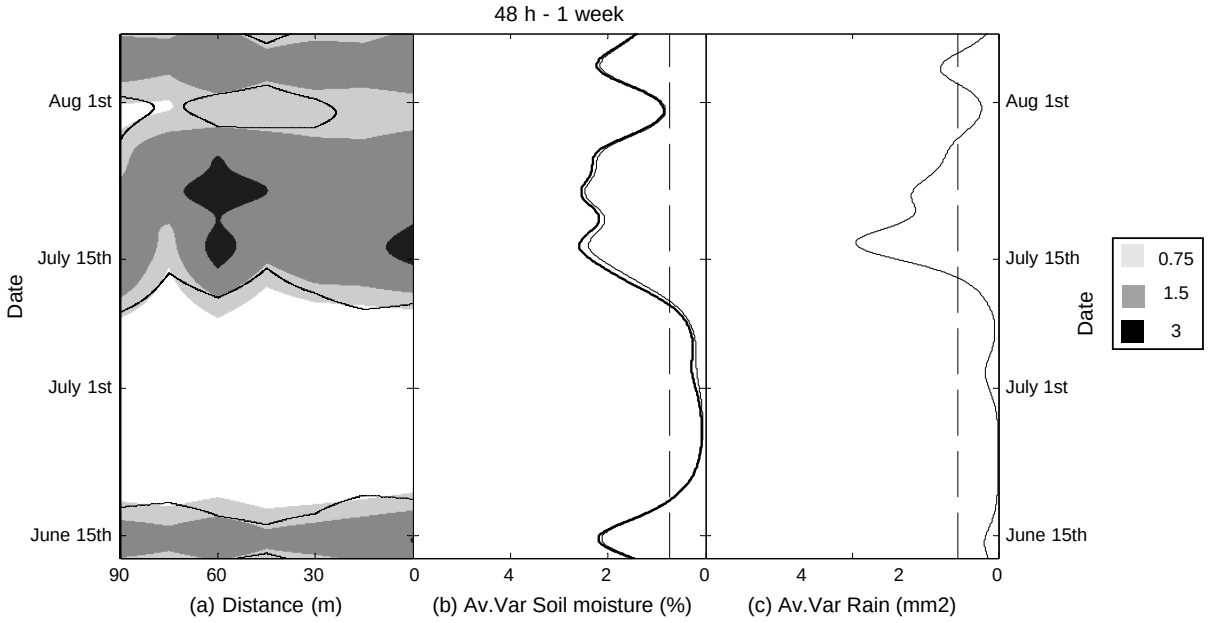


Fig. 4. For band 48 h to 1 week, (a) is the distance–time diagram of soil moisture series. The shaded contours are at normalized variance of 0.75, 1.5 and 3. The bold line is the 95% confidence with lag-1 $\alpha$ coefficient of 1.00. (b) is the scale-averaged wavelet power of soil moisture (bold line is computed from series and thin line is computed from PCA). (c) is the scale-averaged wavelet power of precipitation. Over the dashed line is the 95% confidence with lag-1 $\alpha$ coefficient of 1.00.

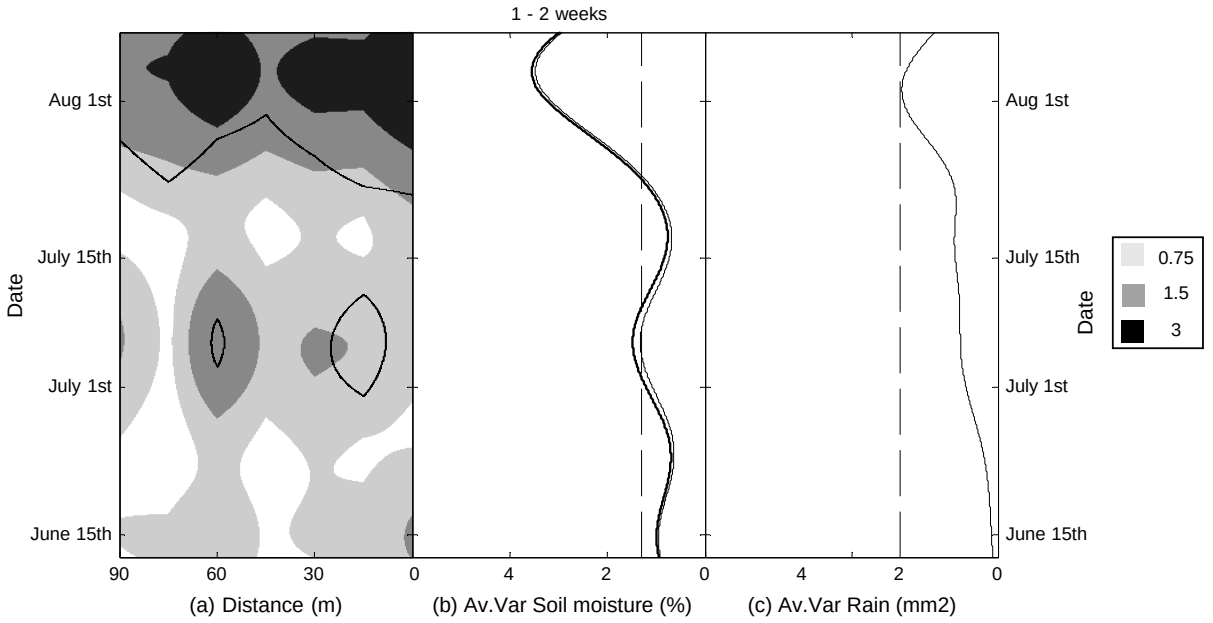


Fig. 5. For band 1–2 weeks, (a) is the distance–time diagram of soil moisture series. The shaded contours are at normalized variance of 0.75, 1.5 and 3. The bold line is the 95% confidence with lag-1 $\alpha$ coefficient of 1.00. (b) is the scale-averaged wavelet power of soil moisture (bold line is computed from series and thin line is computed from PCA). (c) is the scale-averaged wavelet power of precipitation. Over the dashed line is the 95% confidence with lag-1 $\alpha$ coefficient of 1.00.

Table 1
For three predefined bands, i.e. 1–48 h, 48 h to 1 week and 1–2 weeks, SMoist and Prec are the proportion of total variance accounted for by soil and precipitation, respectively

| Band | Proportion of total variance | | Correlation coefficient |
|---|---|---|---|
| | SMoist | Prec | |
| 1–48 h | 0.15 | 0.93 | 0.18 |
| 48 h to 1 week | 0.37 | 0.06 | 0.66 |
| 1–2 weeks | 0.48 | 0.01 | 0.79 |

The correlation coefficient is given between soil moisture and precipitation average variances (Av.Var).

Fig. 3a illustrates the temporal and spatial distribution of soil moisture variance for the 1–48 h band (actually 0.66–49.01 h). Six high power stretched features were averaged in Fig. 3b. Soil moisture peaks of variance directly related to precipitation variance in time scale, but differed in amplitude; the correlation coefficient was 0.42. For example, the highest precipitation variance depicted in Fig. 3c (5.1 $mm^2$, July 17th) did not produce the highest variance in soil moisture (2%). This peak of precipitation variance followed a succession of two rainstorms, totalling 29 mm in 8 h, as shown in Fig. 2a. Later, in July 20th, a smaller precipitation average variance (3.1 $mm^2$) produced a larger soil moisture variance (5%). As shown in Fig. 2a, a rainstorm totalling 15 mm in 4 h occurred at that date, and produced a swift soil moistening. Although surface soil is directly influenced by precipitation, fluctuations in soil water content must depend on several factors as the intensity and distribution of previous and instantaneous rainfall events, the initial soil water content, the evapotranspiration rate, the soil drainage capacity, as well as the season and latitude of the site. In our case, the sequence of rainfalls combined with a high initial water content was responsible of the higher variance observed in July 20th. An important aspect to consider in this analysis is the percentage of total variance expressed by each band, because it enlightens how soil moisture responds to rainfall forcing. Although precipitation remains a process of short duration, the soil moistening response to precipitation lags behind. Thus, in each band, the variance released by precipitation and soil moisture systems should be different. In the 1–48 h band, the variance of soil moisture accounted only for 15% of total variance. On the other hand, 93% of total rainfall variance occurred in this band. Moreover, 81% was located in the first 1–12 h scales. Those results confirmed that rainfall has a short duration effect on soil moisture variance, and that its effects on soil are rather limited at short time scales.

In the 48 h to 1 week band (actually 49.01–170.66 h), the distance–time diagram in Fig. 4a showed again the weak spatial variability between neighbouring series. In Fig. 4b, the average power of soil moisture indicated three features explaining about 2% of total variance (June 15th, July 14th to 20th, and August 4th), each strongly related to the precipitation average power. In the band 48 h to 1 week, soil moisture was mainly influenced by the repeatability of the meteorological systems as indicated by similarities between Fig. 4b and c, and the correlation coefficient of 0.81. Precipitation showed a smaller average power in this band compared to the 1–48 h band, with a maximum peak of only 0.02 $mm^2$. The variance of precipitation in this band accounted only for 6% of total variance. On the other hand, the variance of soil moisture represented 37% of total variance, higher than at short scales (1–48 h). Hence, soil moisture was dependent on precipitation repeatability of the order of 3–7 days.

The 1–2 weeks band (actually 170.66–341.33 h) in Fig. 5 would represent the power features generated by soil effects (i.e. drying and moistening). The variance of soil moisture accounted for 48% of total variance in this band, the highest proportion. One reason for this result is the slow response of the soil to a rainfall. After a rainfall event, most of the soil water apparently drained gradually into deeper soil layers. Precipitation variance accounted for less than 1% of total variance. At that range of scales, soil moisture and precipitation were highly related with a correlation coefficient of 0.89.

## 5. Discussion

Soil moisture varies differently depending on time scale. By partitioning total variance into preferential bands, one can describe how soil moisture relies on the occurrence, the duration and the periodicity of precipitation events. In this study, the wavelet power spectrum of soil moisture showed three distinct ranges

of scales that were then analysed using distance–time diagrams. Anctil and Tape (2004) showed a time-period representation of the precipitation variance that revealed distinct behaviours as the wavelet period increases. Wu et al. (2002); Lauzon et al. (2004) showed that at short scales, soil moisture related mostly to precipitation, while at larger scales, soil moisture was driven by the seasonal cycle effect. In this study, we showed the same effects but at a finer time scale, which refined the comprehension of the precipitation and soil moistening processes. For the 1–48 h scales, soil moisture was linked to rainfall occurrence, intensity and duration, while for the 48 h to 1 week scales, soil moisture was more associated with the periodicity of rainfall events compared to the duration of the dry spells for 2 week scale.

This paper focused on the analysis of soil moisture and precipitation temporal variabilities at very short time scales. Our work refined that of Lauzon et al. (2004) who described the short-term behaviour of soil moisture at temporal scales ranging from 1 to 512 days. Lauzon et al. (2004) showed the short-term impacts of precipitation over surface soil moisture at the 1–16 day scales. By refining the daily scales to hourly, we established that the short-term influence of precipitation on soil moisture can be clarified at the very short hourly scales, i.e. 1–48 h (93% of total variance) than at larger ones, i.e. 48 h to 1 week and 1–2 weeks (only 7% of total variance). In contrast with precipitation, soil moisture variance accounted only for 15% of total variance at hourly scales; but at larger scales, this contribution increased substantially (37% of total variance for the 48 h to 1 week band, and 42% for the 1–2 weeks band). This major difference would result from energy transfer between the two systems: precipitation and soil re-moistening. Precipitation generated high power that was transferred to the soil depending on its drainage conditions. To some extent, soil operated as a low-pass filter redistributing the energy collected from precipitation. This re-allocation of power affected the variance of soil moisture within a frequency band that increased with time scale.

Variability of precipitation influenced the temporal structure and the vertical profile of soil moisture. Wu et al. (2002) measured soil moisture at different depths (0–2 m) and showed an increasing large scale effect of soil moisture with increasing depth. In addition, Lauzon et al. (2004) reported that coherence is particularly significant for periods ranging from 1 to 64 days for soil moisture at a depth of 5 cm, because soil surface was in direct contact with precipitation. This correlation gradually faded off with depth. In our analysis, we also established a close correlation between soil moisture and precipitation at those scales, i.e. 1–2 weeks, with a correlation coefficient of 0.89, whereas correlation was weak for the 1–48 h band.

## 6. Conclusion

Wavelet analysis proved to be a powerful tool for analyzing variance fluctuations in non-stationary time series of rainfall and soil moisture. After reducing data dimensionality by PCA, the wavelet power spectra of precipitation and soil moisture were processed for short time scales, i.e. from 1 h to 2 weeks. Wavelet analysis allowed partitioning the variance into preferential bands. The time series were wavelet decomposed into three sub-series using the power spectra of precipitation and soil moisture, i.e. 1–48 h, 48 h to 1 week, and 1–2 weeks. The precipitation wavelet spectrum revealed high power features related to rainfall events. The PCA soil moisture wavelet spectrum showed similarities with precipitation, and was synchronized with rainfall events.

A distance–time wavelet analysis was processed over the seven time series to compress temporal and spatial variabilities into a single diagram. Spatial variability was weak compared to temporal variability. As expected from the main principal component (94% of explained variance), only small spatial differences were observed between neighbouring series. This homogeneity between series over distance resulted from uniform soil properties. The analysis was performed for predefined ranges of scales in the aim of pointing out the distinct processes peculiar to the precipitation and soil moistening systems. At short scales (1–48 h), soil moisture average variance showed peaks related to precipitation events that were obviously weakly related in intensity (correlation coefficient of 0.42). Most of the variance in soil moisture was found at the larger scales

(85%), i.e. in 48 h to 2 weeks, due to the transfer of energy from precipitation to soil moisture that depended on soil properties. In contrast, precipitation variance concentrated in the 1–48 h range of scales explained 93% of total variance.

This study presented a high resolution analysis (20-min rate observation) of the temporal variations in precipitation and soil re-moistening processes near soil surface (5–25 cm) using wavelet analysis. Wavelet power spectra and distance–time diagrams of soil moisture and precipitation were instrumental in identifying this process.

## Acknowledgements

We are grateful to the Natural Science and Engineering Research Canada and Cultures Dolbec Inc. for their financial contribution, and to Éric Fauveau for collecting field data. Main wavelet analysis routines were provided by C. Torrence and G.P. Compo, available at URL: http://paos.colorado.edu/research/wavelets/.

## References

Anctil, F., Coulibaly, P., 2004. Wavelet analysis of the interannual variability in southern Québec streamflows. American Meteorological Society 17, 163–173.

Anctil, F., Tape, D.G., 2004. An exploration of artificial neural network rainfall-runoff forecasting combined with wavelet decomposition. Journal of Environmental Engineering and Science 3, S121–S128.

Cosh, M.H., Brutsaert, W., 2003. Microscale structural aspects of vegetation density variability. Journal of Hydrology 276, 128–136.

Entin, J.K., Robock, A., Vinnikov, K.Y., Hollinger, S.E., Liu, S., Namkhai, A., 2000. Temporal and spatial scales of observed soil moisture variations in the extratropics. Journal of Geophysical Research 105 (D9), 11865–11877.

Farge, M., 1992. Wavelet transforms and their applications to turbulence. Annual Review of Fluid Mechanics 24, 395–457.

Georgakakos, K.P., Baumer, O.W., 1996. Measurement and utilization of on-site soil moisture data. Journal of Hydrology 184, 131–152.

Joliffe, I,T., 2002. Principal component analysis, Springer Series in Statistics, second ed. 2002 487 p.

Kumar, P., Foufoula-Georgiou, E., 1997. Wavelet analysis for geophysical applications. Reviews of Geophysics 35, 385–412.

Labat, D., Ababou, R., Mangin, A., 2000. Rainfall-runoff relations for Karstic springs - part II: continuous wavelet and discrete orthogonal multiresolution analyses. Journal of Hydrology 238, 149–178.

Lafrenière, M., Sharp, M., 2003. Wavelet analysis of inter-annual variability in the runoff regimes of glacial and nival stream catchments, Bow Lake, Alberta. Hydrological Processes 17 (6), 1093–1118.

Lark, R.M., Webster, R., 1999. Analysis and elucidation of soil variation using wavelets. European Journal of Soil Science 50, 185–208.

Lark, R.M., Webster, R., 2001. Changes in variance and correlation of soil properties with scale and location: Analysis using an adapted maximal overlap discrete wavelet transforms. European Journal of Soil Science 52, 547–562.

Lauzon, N., Anctil, F., Petrinovic, J., 2004. Characterization of soil moisture conditions at temporal scales from few days to annual. Hydrological Processes 18, 3235–3254.

Malamud, B.D., Turcotte, D.L., 1999. Self-affine time series: I. Generation and analyses. Advances in Geophysics 40, 1–90.

Morari, F., Giardini, L., 2002. Irrigation automation with heterogeneous vegetation: the case of the Padova botanical garden. Agricultural Water Management 55, 183–201.

Nicholls, N., 2001. The insignificance of significance testing. Bulletin of the American Meteorology Society 81 (5), 981–986.

Si, B.C., Farell, R.E., 2004. Scale-dependent relationship between wheat yield and topographic indices: a wavelet approach. Soil Science Society of America Journal 68, 577–587.

Smith, L.C., Turcotte, D.L., Isacks, B.L., 1998. Stream flow characterization and feature detection using a discrete wavelet transform. Hydrological Processes 12 (2), 233–249.

Torrence, C., Compo, G.P., 1998. A practical guide to wavelet analysis. Bulletin of the American Meteorological Society 79, 61–78.

Vinnikov, K.Y., Robock, A., Speranskaya, N.A., Schlosser, C.A., 1996. Scales of temporal and spatial variability of midlatitude soil moisture. Journal of Geophysical Research 101 (D3), 7163–7174.

Wu, W., Geller, M.A., Dickinson, R.E., 2002. The response of soil moisture to long-term variability of precipitation. Journal of Hydrometeorology 3, 604–613.